

Accretion of planetary matter and the lithium problem in the 16 Cygni stellar system

Morgan Deal^{1,3}, Olivier Richard¹, and Sylvie Vauclair^{2,3}

¹ Laboratoire Univers et Particules de Montpellier (LUPM), UMR 5299, Université de Montpellier, CNRS, Place Eugène Bataillon 34095 Montpellier Cedex 5 FRANCE

² Université de Toulouse, UPS-OMP, IRAP, France

³ CNRS, IRAP, 14 avenue Edouard Belin, 31400 Toulouse, France
e-mail: morgan.deal@umontpellier.fr

May 31, 2022

ABSTRACT

Context. The 16 Cygni system is composed of two solar analogs with similar masses and ages. A red dwarf is in orbit around 16 Cygni A whereas 16 Cygni B hosts a giant planet. The abundances of heavy elements are similar in the two stars but lithium is much more depleted in 16 Cygni B than in 16 Cygni A, by a factor of at least 4.7.

Aims. The interest of studying the 16 Cygni system is that the two stars have the same age and the same initial composition. The presently observed differences must be due to their different evolution, related to the fact that one of them hosts a planet contrary to the other one.

Methods. We computed models of the two stars which precisely fit the observed seismic frequencies. We used the Toulouse Geneva Evolution Code (TGECE) that includes complete atomic diffusion (including radiative accelerations). We compared the predicted surface abundances with the spectroscopic observations and confirmed that another mixing process is needed. We then included the effect of accretion-induced fingering convection.

Results. The accretion of planetary matter does not change the metal abundances but leads to lithium destruction which depends on the accreted mass. A fraction of earth mass is enough to explain the lithium surface abundances of 16 Cygni B. We also checked the beryllium abundances.

Conclusions. In the case of accretion of heavy matter onto stellar surfaces, the accreted heavy elements do not remain in the outer convective zones but they are mixed downwards by fingering convection induced by the unstable μ -gradient. Depending on the accreted mass, this mixing process may transport lithium down to its nuclear destruction layers and lead to an extra lithium depletion at the surface. A fraction of earth mass is enough to explain a lithium ratio of 4.7 in the 16 Cygni system. In this case beryllium is not destroyed. Such a process may be frequent in planet host stars and should be studied in other cases in the future.

1. Introduction

The bright solar analogs 16 Cygni A (HD 186408, HR 7503) and 16 Cygni B (HD 186427, HR 7504) represent a very interesting stellar system for many reasons. While a red dwarf, 16 Cygni C, is in orbit around the first component 16 Cygni A (Turner et al. 2001; Patience et al. 2002), the second component, 16 Cygni B, hosts a giant jovian planet with minimum mass $1.5 M_{Jup}$ located on an eccentric orbit ($e=0.63$), with an orbital period 800.8 days (Cochran et al. 1997). The two main stars are separate enough, with an orbital period longer than 18,000 years (Hauser & Marcy 1999), to be studied in the same way as two isolated stars, with no common dynamical effects.

This situation allows for precise differential studies between a planet-host star and a non-planet-host star with similar birth conditions. The presence of the red dwarf around 16 Cygni A may be the reason why no accretion disk could have developed around it, whereas a planetary disk remained around 16 Cygni B, including the observed giant planet, and probably smaller still unobserved bodies.

The two main stars of the 16 Cygni system have been studied in many ways, using spectroscopy, interferometry, and asteroseismology. The abundances of the heavy elements in these two stars are very close. Although a very small difference has been claimed by Ramírez et al. 2011 and Tucci Maia et al. 2014, Schuler et al. (2011) find them indistinguishable. On the other

hand, the surface lithium abundance of 16 Cygni B is smaller than that of 16 Cygni A by at least a factor 4.7 (King et al. 1997). These observations lead to several open questions, which remain to be answered for a better understanding of these stars.

The interest of this study is that these stars have the same birth site and the same age, with masses of the same order, so that their past evolution is similar for most aspects. The observed differences between them must basically be due to the presence of a planetary disk around B. For this reason, the detailed study of this stellar system helps understanding the differences between stars with and without planetary disks.

The present paper is motivated by two considerations. The first one is that, in all previous modelling of these two stars, atomic diffusion including the radiative acceleration on each element was not introduced. At the present time, most stellar evolution codes include the atomic diffusion of helium (without radiative accelerations), some of them also include it for heavy elements, but very few consider the radiative accelerations.

The second consideration refers to the consequences of the accretion of heavy matter onto stars, which may occur when the star has a planetary disk. Many studies and past publications assume that the accreted matter remains inside the outer stellar convective zone, so that accretion can lead to an increase of the heavy elements abundances, as well as the lithium one. This assumption is not valid, as shown in detail by Vauclair (2004), Garaud (2011), Théado et al. (2012), and Deal et al. (2013). When

heavy matter falls onto the star, it creates an inverse gradient of molecular weight which leads to a double-diffusive instability now called fingering (or thermohaline) convection. The heavy elements are mixed downwards until the mean molecular weight gradient becomes nearly flat. In most cases, no signature of the accreted heavy elements remains at the surface. Meanwhile, as computed in detail by Théado & Vauclair (2012), the induced mixing may lead to an extra lithium depletion in the star. As a consequence, the accretion of heavy matter cannot lead to any increase of lithium at the surface of a star, but on the contrary it may lead to a decrease of its observed abundance.

The observational results on the two main stars 16 Cygni A and B are presented in Section 2 together with a discussion of the still unsolved questions. In section 3, we present models of 16 Cygni A and B which fit the observed seismic frequencies. We compare the parameters of these models with the previously published ones. The surface abundances of heavy elements and lithium which are obtained after diffusion in these models are discussed in section 4. Finally, in section 5, we show that the accretion of metal rich planetary matter at the beginning of the main sequence on 16 Cygni B may explain the lithium difference between the two stars. A summary and discussion of all these results are given in section 6.

2. Observational constraints

The position in the sky of the 16 Cygni system allowed seismic observations with the *Kepler* satellite. More than 40 modes of degree $l=0, 1, 2$ and 3 could be detected. Analyses with the Asteroseismic Modelling Portal (AMP) and comparisons with other seismic studies could lead to precise values of the masses, radius and ages of the two stars (Metcalf et al. 2012). Moreover, the seismic observations allowed measurements of their stellar rotation periods (Davies et al. 2015).

The effective temperatures and gravities of the two stars were derived from spectroscopic observations (e.g. Ramírez et al. 2011; Schuler et al. 2011; Tucci Maia et al. 2014). We must however insist on the fact that asteroseismology leads to the $\log g$ value with a much better precision than spectroscopy. As will be shown in section 3, all the models which closely fit the observed seismic frequencies, even if they have different masses, radii, helium abundances, ages, luminosities, have the same $\log g$ value with a precision of 0.001. The determinations of the bolometric magnitudes (Torres 2010) and Hipparcos parallaxes (van Leeuwen 2007) lead to precise values of the luminosities of the two stars. They are also bright enough for their radii to be determined by interferometric techniques (White et al. 2013). The results are given in Table 1.

Detailed determination of their element abundances have been given by several authors. Using high signal-to-noise ratio spectroscopy with the 10m Keck 1 telescope and HIRES echelle spectrograph, Schuler et al. (2011) determined the abundance of 15 heavy elements in both stars and found them indistinguishable. On the other hand, Ramírez et al. (2011) and Tucci Maia et al. (2014) claim that 16 Cygni A is slightly more metal rich than 16 Cygni B, using high resolution, high signal to noise ratio spectra obtained with the R.G. Hull coude spectrograph on the 2.7m Harlan Smith telescope at Mc Donald Observatory.

A more striking difference between the two stars, confirmed by all spectroscopic observations, is that the star holding a planet, 16 Cygni B, has an abundance of lithium at least four times smaller than the one which has no planet (Friel et al. 1993; King et al. 1997). While both stars are lithium depleted compared to F stars and to the meteoritic value, detailed measure-

Table 1. Properties of 16 Cygni A and B from literature

| | 16 Cygni A | 16 Cygni B |
|----------------------------|-------------------------|-------------------------|
| $T_{\text{eff}}(\text{K})$ | 5825 ± 50^a | 5750 ± 50^a |
| | 5813 ± 18^b | 5749 ± 17^b |
| | 5796 ± 34^c | 5753 ± 30^c |
| | 5839 ± 42^d | 5809 ± 39^d |
| | 5830 ± 7^f | 5751 ± 6^f |
| $\log g$ | 4.33 ± 0.07^a | 4.34 ± 0.07^a |
| | 4.282 ± 0.017^b | 4.328 ± 0.017^b |
| | 4.38 ± 0.12^c | 4.40 ± 0.12^c |
| | 4.30 ± 0.02^f | 4.35 ± 0.02^f |
| [Fe/H] | 0.096 ± 0.026^a | 0.052 ± 0.021^a |
| | 0.104 ± 0.012^b | 0.061 ± 0.011^b |
| | 0.07 ± 0.05^c | 0.05 ± 0.05^c |
| | 0.101 ± 0.008^f | 0.054 ± 0.008^f |
| A(Li) | 1.27 ± 0.05^i | $\leq 0.6^i$ |
| A(Be) | 0.99 ± 0.08^j | 1.06 ± 0.08^j |
| Mass (M_{\odot}) | 1.05 ± 0.02^b | 1.00 ± 0.01^b |
| | 1.07 ± 0.05^d | 1.05 ± 0.04^d |
| | 1.11 ± 0.02^g | 1.07 ± 0.02^g |
| Radius (R_{\odot}) | 1.218 ± 0.012^d | 1.098 ± 0.010^d |
| | 1.22 ± 0.02^e | 1.12 ± 0.02^e |
| | 1.243 ± 0.008^g | 1.127 ± 0.007^g |
| Luminosity (L_{\odot}) | 1.56 ± 0.05^g | 1.27 ± 0.04^g |
| Age (Gyrs) | $7.15^{+0.04b}_{-1.03}$ | $7.26^{+0.69b}_{-0.33}$ |
| | 6.9 ± 0.3^g | 6.7 ± 0.3^g |
| Z_i | 0.024 ± 0.002^g | 0.023 ± 0.002^g |
| Y_i | 0.25 ± 0.01^g | 0.25 ± 0.01^g |
| $v \sin i$ (km.s $^{-1}$) | 2.23 ± 0.07^h | 1.27 ± 0.04^h |
| P_{rot} (days) | $23.8^{+1.5h}_{-1.8}$ | $23.2^{+11.5h}_{-3.2}$ |
| Planet detected | no | yes k |

Notes. ^(a) Ramírez et al. (2009) ; ^(b) Ramírez et al. (2011) ; ^(c) Schuler et al. (2011) ; ^(d) White et al. (2013), seismic determination ; ^(e) White et al. (2013), interferometric determination ; ^(f) Tucci Maia et al. (2014) ; ^(g) Metcalfe et al. (2012) ; ^(h) Davies et al. (2015) ; ⁽ⁱ⁾ King et al. (1997) ; ^(j) Deliyannis et al. (2000) ; ^(k) Cochran et al. (1997)

ments show that 16 Cygni A is slightly less depleted than the Sun ($\log N(\text{Li}) = 1.27$ compared to 1.05 for the Sun), whereas 16 Cygni B is more depleted ($\log N(\text{Li}) < 0.60$). On the other hand, Deliyannis et al. (2000) found that the Be and B abundances are the same in the two stars, in the limits of the uncertainties.

3. Asteroseismic studies and stellar models including radiative accelerations

3.1. Stellar models

We used the Toulouse Geneva Evolution Code (TGECE) to compute stellar models that fit the seismic observations of 16 Cygni A and B. This code performs complete computations of atomic diffusion, including radiative accelerations, for 21 species, namely 12 elements and their main isotopes: H, ^3He , ^4He , ^6Li , ^7Li , ^9Be , ^{10}B , ^{12}C , ^{13}C , ^{14}N , ^{15}N , ^{16}O , ^{17}O , ^{18}O , ^{20}Ne , ^{22}Ne , ^{24}Mg , ^{25}Mg , ^{26}Mg , ^{40}Ca and ^{56}Fe (Théado et al. 2012).

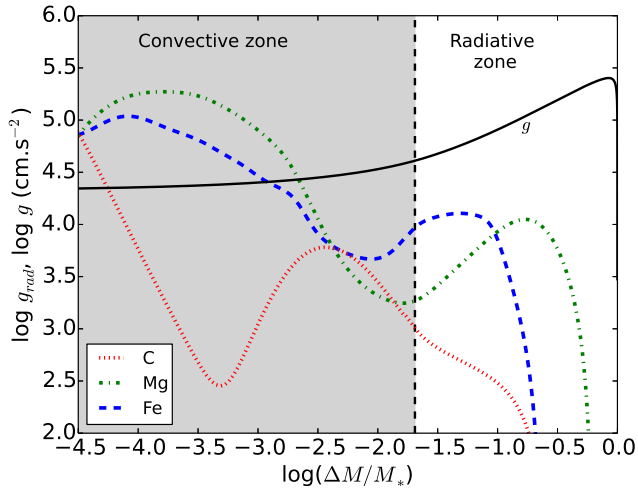


Fig. 1. Profiles of the radiative accelerations on three elements Fe, Mg and C as a function of the mass fraction in 16 Cygni A.

The diffusion coefficients used in the code are those derived by Paquette et al. (1986).

The Rosseland opacities are recalculated inside the model, at each time step and at every mesh point, using OPCODE v3.3 and data from Seaton (2005), to take into account the local chemical composition. In this way, the stellar structure is consistently computed all along the evolutionary tracks, as well as the individual radiative accelerations of C, N, O, Ne, Mg, Ca, and Fe. This is done by using the improved semi-analytical prescription proposed by Alecian & Leblanc (2004). A more detailed discussion of these computations are given in Deal et al. (2015) (in prep).

The equation of state used in the code is the OPAL2001 equation (Rogers & Nayfonov 2002). The nuclear reaction rates are from the NACRE compilation (Angulo 1999). The mixing length formalism is used for the convective zones with a mixing length parameter of 1.8, as needed to reproduce solar models.

As an example, Fig. 1 displays the g_{rad} profiles for C, Mg and Fe compared to gravity for one of the computed models of 16 Cygni A. This model is precisely the one which fits the best the asteroseismic observations, as will be discussed in section 3.2. The dashed vertical line represents the position of the surface convective zone. We see that below the convective zone g_{rad} is at least 1/3 smaller than g , so that the effect of the radiative accelerations is small and generally negligible inside these stars.

3.2. Best models from asteroseismic fits

The stellar oscillation modes were derived for each model using the PULSE code (Brassard & Charpinet 2008). The frequencies were corrected for surface effects in the way proposed by Kjeldsen et al. (2008).

We computed models with masses ranging from 1.05 to 1.14 M_{\odot} . The initial helium mass fraction Y_i was varied from 0.245 to 0.26 and the heavy elements mass fraction Z_i from 0.023 to 0.025 (initial mass fraction of all elements heavier than helium).

Evolutionary tracks computed for two different initial compositions $Y_i=0.25$; $Z_i=0.024$ and $Y_i=0.26$; $Z_i=0.024$ are presented in Fig. 2. The error boxes are from Ramírez et al. (2009) (red dashed lines), Ramírez et al. (2011) (green dotted-dashed

lines), Schuler et al. (2011) (blue dotted lines) and Tucci Maia et al. (2014) (black dotted lines). The black thick lines indicate the models which have a radius consistent with the interferometric determinations of White et al. (2013).

The observational uncertainties on the oscillation frequencies for $l = 0$ to $l = 2$ modes lie between 0.1 to 1.45 μHz (Metcalfe et al. 2012). The derived large separations $\Delta\nu$ for 16 Cygni A and for 16 Cygni B are respectively $\Delta\nu_{obs} = 103.56 \pm 0.10 \mu\text{Hz}$ and $\Delta\nu_{obs} = 117.17 \pm 0.10 \mu\text{Hz}$. The models which have large separations that fit these values are represented by blue dots in Fig. 2. They include the corrections for surface effects as proposed by Kjeldsen et al. (2008). Neglecting this effect would lead to models slightly above the blue dots, with a small difference in age of average 150 million years.

Note that all the models presented on Fig. 2 lie on horizontal lines, which means that they all have about the same surface gravity. This is a well known result of asteroseismology. The asymptotic treatment of the oscillations (e.g. Tassoul 1980) shows that the large separation $\Delta\nu$ directly gives the average stellar density. In the range of our possible models, the variations in radii are small so that $\log g$ is also nearly constant. In other words, if any parameter of the model is modified, e.g. the initial Y value, the other parameters like age adjust to obtain a model with the same large separation, and thus the same gravity. Spectroscopy is only used in our description to constrain the effective temperatures.

The uncertainty on the $\log g$ values derived from the observed seismic frequencies for each track is of the order of 10^{-3} . This is the uncertainty on the position of the models represented by blue dots in Fig. 2. The corresponding error bars would lie inside the printed symbols. Note that the seismic $\log g$ values lie outside the ranges given by Ramírez et al. (2011) (see Fig. 2) which suggests that their uncertainties are underestimated.

We then derived the best of all these models for both stars. We first did it independently for each Y_i value. The best models (represented by squares) were selected first because of the best fit of their small separations $\delta\nu_{0,2}$ with the observed ones, second because of the best fit of their echelle diagrams with the observed ones, according to χ^2 minimisations performed between the observed and the modelled frequencies.

When compared with spectroscopic observations (see Fig. 2), it is clear that for $Y_i=0.25$ the best models lie inside the Schuler et al. (2011) box for 16 Cygni A only, not for 16 Cygni B, and that they are outside the Tucci Maia et al. (2014) ones for both stars. On the contrary, for $Y_i=0.26$ the best models lie inside all the boxes for both stars. For this reason, we find that the $Y_i=0.26$ value is more probable than the $Y_i=0.25$ one.

The echelle diagrams corresponding to the best case computed with $Y_i=0.26$ are presented in Fig. 3 for 16 Cygni A (left panel) and 16 Cygni B (right panel). We can see that the fits between the computed and observed frequencies are very good for both stars. The corresponding stellar masses are $M_A = 1.10 M_{\odot}$ and $M_B = 1.06 M_{\odot}$.

These values, as well as the other parameters obtained for these best models, are given in Table 2. The uncertainties which are given in this table correspond to the possible range of parameters of all the computed models which have large and small separations in the observational uncertainties.

We must notice that the present surface helium abundances derived from these computations are slightly subsolar, whereas the spectroscopic parameters given in the literature have been computed using a solar helium value. It would be interesting in the future to iterate with spectroscopists and see how such a he-

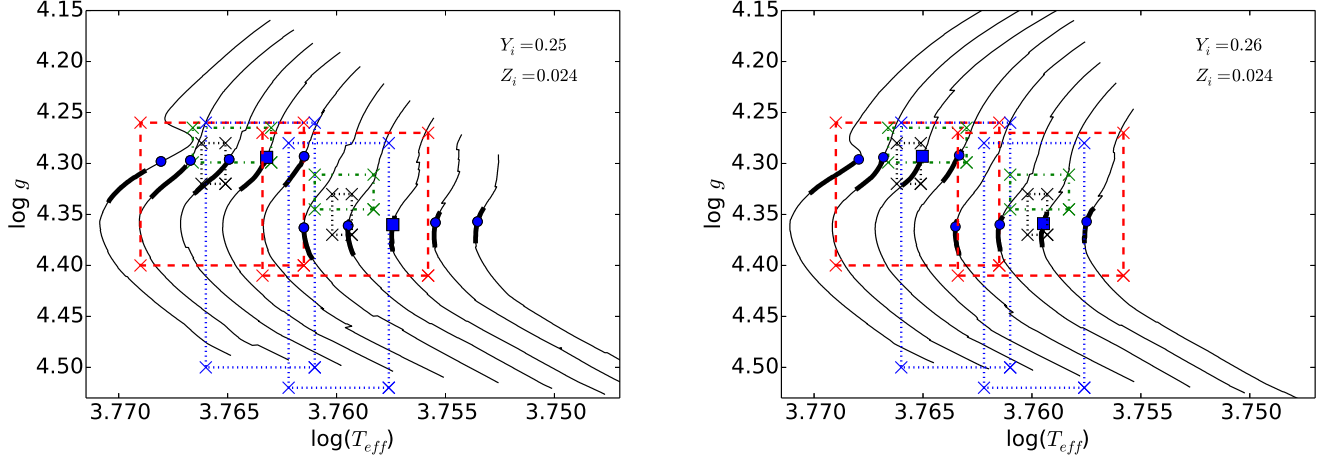


Fig. 2. Evolutionary tracks for models from 1.05 to 1.14 M_{\odot} (from right to left) with $Z_i = 0.024$ and $Y_i = 0.25$ (left panel) and evolutionary tracks for models from 1.05 to 1.12 M_{\odot} (from right to left) with $Z_i = 0.024$ and $Y_i = 0.26$ (right panel). The error boxes are those of Ramírez et al. (2009) (red dashed lines), Ramírez et al. (2011) (green dotted-dashed lines), Schuler et al. (2011) (blue dotted lines) and Tucci Maia et al. (2014) (black dotted lines). The blue dots indicate models with the right large separation, taking Kjeldsen et al. (2008) corrections into account. The blue squares correspond to models which also have the right small separations and fit the best the Echelle Diagram. The black thick segments on each line indicate the models which have radii consistent with the interferometric determinations of White et al. (2013).

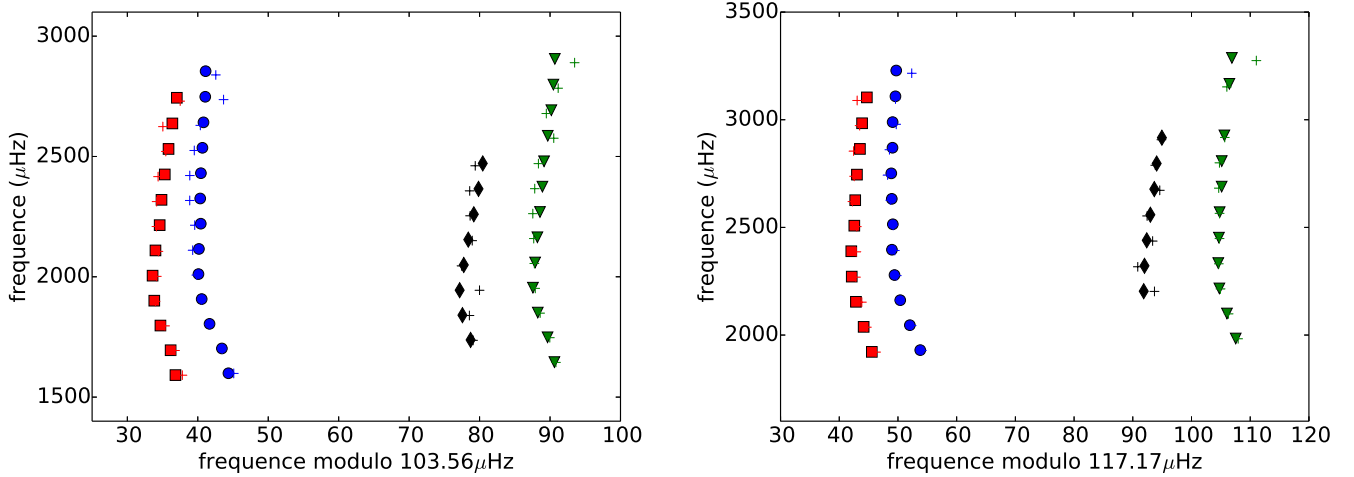


Fig. 3. Echelle diagrams for 16 Cygni A (left panel) and 16 Cygni B (right panel). The observed frequencies are represented by crosses. The frequencies computed for the models with $Y=0.26$ and $Z=0.024$ are represented by blue dots ($l=0$), green triangles ($l=1$), red squares ($l=2$) and black diamonds ($l=3$).

lithium difference could influence the derived effective temperature range.

4. Heavy elements and lithium abundances in 16 Cygni A and B, observational and theoretical discussions

4.1. Discussion of the spectroscopic observations

The abundances of heavy elements in 16 Cygni A and B have been a subject of debate for 15 years. Deliyannis et al. (2000) reported an iron overabundance larger in 16 Cygni B than in 16 Cygni A, which has not been confirmed by more recent papers. Whereas Schuler et al. (2011) could not see any difference between 16 Cygni A and B for the abundances of heavy elements,

Ramírez et al. (2011) and Tucci Maia et al. (2014) claimed that the heavy elements are overabundant in 16 Cygni A compared to 16 Cygni B. In any case, all observers agree that lithium is more depleted in 16 Cygni B than in 16 Cygni A by a large factor. Lithium has not been detected in B whereas its abundance in A is slightly larger than that of the Sun, such a difference between these very similar stars is difficult to account for using traditional explanations of lithium depletion in G stars.

In the following, we discuss the influence of atomic diffusion and mixing on the lithium and heavy elements abundances and we show how the lithium difference between the two stars may be explained. We also discuss the consequences of these effects for heavy elements.

Table 2. Properties of 16 Cygni A and B from this work

| | 16 Cygni A | 16 Cygni B |
|----------------------------|-------------------|-------------------|
| $T_{\text{eff}}(\text{K})$ | 5821 ± 25 | 5747 ± 25 |
| $\log g$ | 4.293 ± 0.001 | 4.359 ± 0.001 |
| Mass (M_{\odot}) | 1.10 ± 0.01 | 1.06 ± 0.01 |
| Radius (R_{\odot}) | 1.239 ± 0.010 | 1.129 ± 0.010 |
| Luminosity (L_{\odot}) | 1.58 ± 0.03 | 1.25 ± 0.03 |
| Age (Gyrs) | 6.400 ± 0.025 | 6.400 ± 0.025 |
| Z_i | 0.024 | 0.024 |
| Y_i | 0.26 | 0.26 |
| Z_{surf}^a | 0.0221 | 0.0223 |
| Y_{surf}^a | 0.2226 | 0.2265 |

Notes. ^(a) Values at the age of best models ;

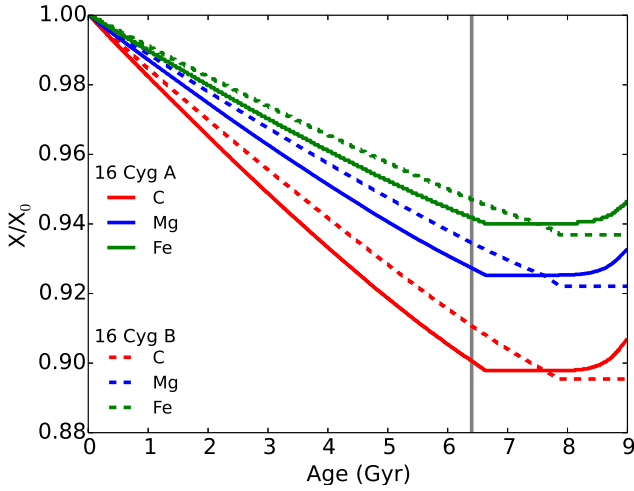


Fig. 4. Abundance evolution of C, Mg and Fe in our best models of 16 Cygni A and B, under the influence of atomic diffusion below the convective zone, when no mixing is taken into account.

4.2. Influence of atomic diffusion on the abundances of heavy elements and lithium

Our models include the computation of detailed atomic diffusion for a large number of elements, as discussed in Section 3.1. Figure 4 presents the surface abundance evolution for three of these elements, C, Mg, and Fe, in both 16 Cygni A and B. As the mass of 16 Cygni A is larger than that of 16 Cygni B, the convective zone is smaller and the diffusion processes faster. As a consequence, the surface abundances predicted by the models are larger in 16 Cygni B than in 16 Cygni A by ~ 0.002 dex at the age of our best models (vertical line). Later on in the evolution, around 8 Gyrs, the situation is reversed because the surface convective zone sinks more quickly in the more massive star. This occurs however in models which are too old to account for the observations.

Figure 5 displays the abundance profiles for the same three elements C, Mg and Fe in the best models for 16 Cygni A and B. The bottom of the convective zones are shown as vertical dashed lines. The difference of heavy elements abundances is due to the difference in surface convective zone depth which is deeper in 16 Cygni B than A (grey dashed line).

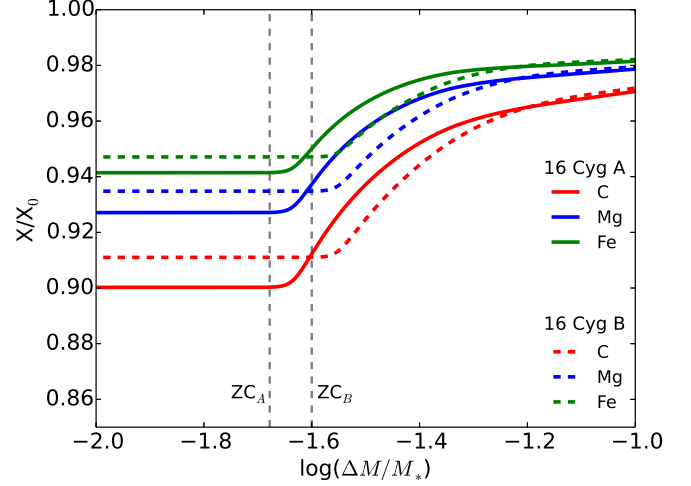


Fig. 5. Abundance profiles C, Mg and Fe inside the stars in the same conditions as for Fig. 4.

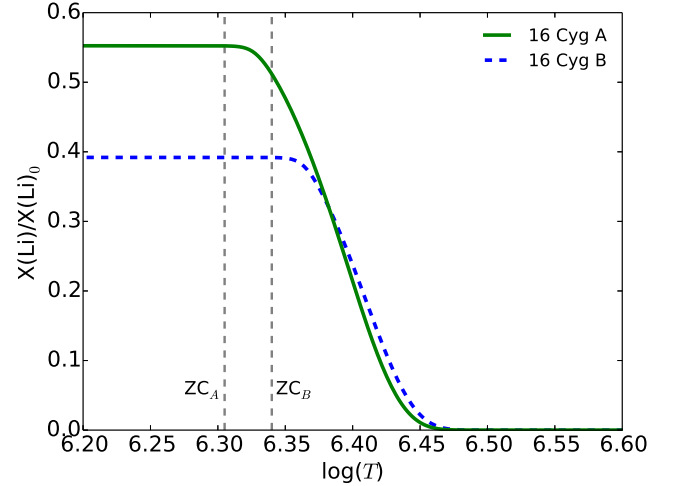


Fig. 6. Abundance profiles of lithium in the same conditions as for Fig. 4.

Atomic diffusion coupled with nuclear destruction has also an impact on the abundance of ^7Li (see Fig. 6). In this case, the final abundance of ^7Li is smaller in 16 Cygni B than in 16 Cygni A. This is not enough to account for the observations. First lithium is depleted in 16 Cygni A by a factor less than two, whereas in the real star it is depleted by 100. Second the depletion ratio between the two star is only ~ 1.4 whereas the observations show a ratio of at least 4.7. Extra mixing below the convective zones is definitively needed to account for the observations.

4.3. Mixing processes below the outer convective zone

A very large number of papers have been published since about 30 years on the subject of the mixing processes which may occur below the convective zones of solar type stars and result in lithium destruction in their outer layers. The most common one

is rotational-induced mixing (e.g. Vauclair 1988; Pinsonneault et al. 1990; Charbonnel et al. 1992, 1994; Castro et al. 2009).

The rotation periods of 16 Cygni A and B have recently been measured with high precision using asteroseismology (Davies et al. 2015). They are very close, 23.8 days for A, 23.2 days for B, with a difference smaller than the uncertainties. The authors have also determined their inclination angles, 56 degrees for A, 36 degree for B. Using the interferometric radius, the resulting $v \sin i$ is 2.23 km.s^{-1} for A and 1.27 km.s^{-1} for B.

When studying rotational-induced mixing, it appears that the efficiency of the mixing is related to the local linear rotation velocity in such a way that it increases with radius. The bottom of the convective zone lies at a larger radius in A than in B, but the mixing is also more efficient. Simple expressions of the mixing diffusion coefficients (e.g. Zahn 1992) include the factor $(\Omega^2 R^3 / GM)$, which is about 1.3 larger for 16 Cygni A than for 16 Cygni B. As already discussed by Deliyannis et al. (2000), it does not seem possible to account for the lithium abundance ratio between A and B by such a simple process. It would not be realistic to invoke a larger rotational-induced mixing effect in B than in A, just to account for the observations. Another process is definitively needed.

In the present paper, we do not intend to discuss all these processes. We only simulate turbulent mixing by using a turbulent diffusion coefficient adjusted to obtain a lithium destruction by a factor 100 in 16 Cygni A and we used the same one to deduce the lithium destruction in 16 Cygni B. As in the simulations of Richer et al. (2000) we used a simple form $D_T = \omega D(\text{He}) \left(\frac{\rho_0}{\rho}\right)^n$ with $n = 3$, $\omega = 325$, $D(\text{He})$ the helium diffusion coefficient and ρ_0 the density at the bottom of the outer convective zone.

Figure 7 displays the resulting surface lithium abundance evolution in the two stars (green solid line and blue dashed line). As expected, lithium is more destroyed in 16 Cygni B than in 16 Cygni A, but only by a factor 2.9, not enough to account for the observations of an abundance ratio larger than 4.7 at the age of the stars.

Meanwhile, the abundance of heavy elements is also modified, but in no way the abundances in 16 Cygni B may become smaller than in 16 Cygni A (see Fig. 8).

5. Fingering convection and lithium destruction induced by planetary accretion

Let us now come back on the fact that the star 16 Cygni B hosts a giant planet whereas 16 Cygni A does not. As discussed in the introduction, the red dwarf which orbits 16 Cygni A may be the reason for the fact that the main star could not develop any planetary disk.

In such a situation, it is quite possible that in its early period on the main sequence 16 Cygni B could accrete some matter from its planetary disk, which could not occur for 16 Cygni A. As discussed by (Théado & Vauclair 2012), the accretion of heavy planetary matter onto a stellar surface builds an unstable compositional gradient at the bottom of the surface convective zone which triggers fingering (thermohaline) convection. This mixing leads to complete dilution of the heavy matter inside the star, so that no signature appears at the surface for the heavy elements. On the other hand, it may lead to extra lithium depletion due to its mixing down to the destruction layers.

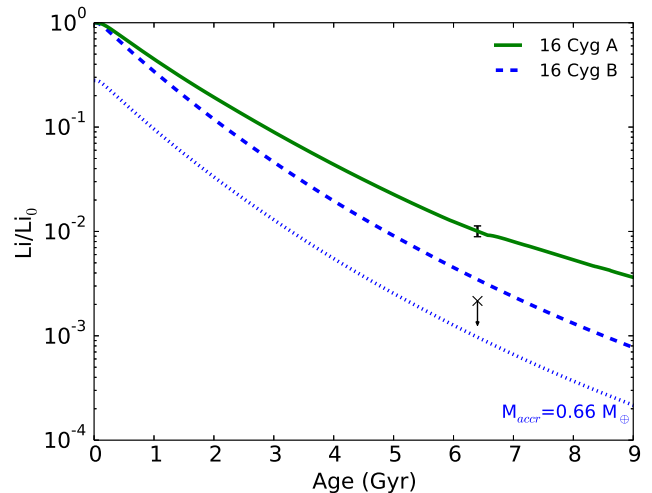


Fig. 7. Evolution of lithium surface abundances including a mixing at the bottom of the outer convective zone needed to reproduce 16 Cygni A abundance in the two models (green solid line and blue dashed line) (Section 4.3). Evolution of lithium surface abundances including accretion of $0.66 M_{\text{J}}$ for 16 Cygni B (blue dotted line) at the beginning of the main sequence but with the same mixing as before (Section 5). Abundances determined using observations from King et al. (1997) are represented by black crosses.

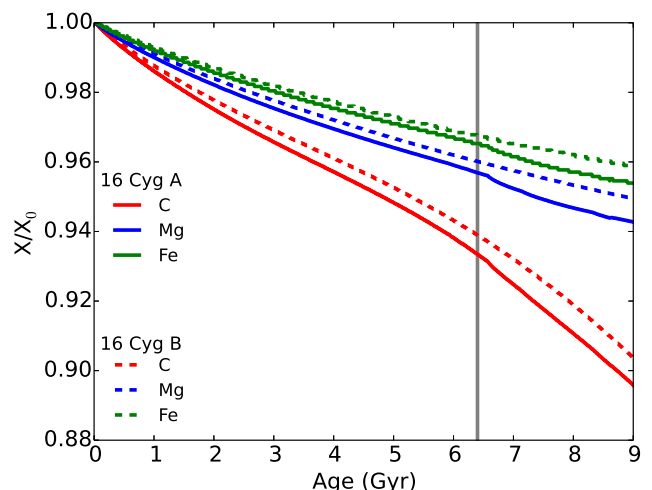


Fig. 8. Abundance evolution of C, Mg and Fe in our best models of 16 Cygni A and B, under the influence of atomic diffusion below the convective zone, when a mixing is taken into account.

5.1. Computations of fingering convection

Fingering convection may occur in stars every time a local accumulation of heavy elements appears in the presence of a stable temperature gradient. It happens in particular in the case of the accretion of planetary matter (Vauclair 2004; Garaud 2011; Deal et al. 2013).

Fingering convection is characterised by the so-called density ratio R_0 which is the ratio between the thermal and μ -gradients:

$$R_0 = \frac{\nabla - \nabla_{ad}}{\nabla_{\mu}}.$$

The instability can only develop if this ratio is larger than one, and smaller than the Lewis number, ratio of the thermal to the molecular diffusivities. In this case a heavy blob of fluid falls down inside the star and keeps falling because it exchanges heat more quickly than particles with the surroundings. If R_0 is smaller than one, the region is dynamically convective (Ledoux criterium) and if it is larger than the Lewis number the region is stable.

Various analytical treatments of fingering convection in stars were given in the past, leading to mixing coefficients which could differ by orders of magnitude (Ulrich 1972; Kippenhahn et al. 1980). More recently, 2D and 3D numerical simulations were performed, converging on coefficients of similar orders (Denissenkov 2010; Traxler et al. 2011).

Here we used the recent prescription given by Brown et al. (2013), which has been confirmed by the 3D simulations of Zemska et al. 2014.

5.2. Impact of accretion-induced fingering convection on the lithium abundance of 16 Cygni B

We computed stellar models of 16 Cygni B with the assumption of accretion of planetary matter at the beginning of the main sequence phase. These models included the treatment of fingering convection in the case of an inversion of the mean molecular weight gradient. We tested different accretion masses to characterize their impact on the lithium surface abundance due to fingering convection. In these computations, the accreted matter was supposed to have an earth-like chemical composition (Allègre et al. 1995). Changing the relative abundances of the accreted heavy elements have a very small impact, only due to the fact that their contribution to the mean molecular weight may be slightly different. For example, decreasing the iron abundance by a factor two compared to other elements modifies the computed accretion mass by less than 10%.

Abundance profiles of lithium after the accretion of various masses of planetary matter are presented in Fig. 9. The blue solid curve represents the lithium profile without accretion, the green dashed curve represents the lithium profile after an accretion of $0.6 M_{\oplus}$, the red dotted curve represents the lithium profile after an accretion of $0.66 M_{\oplus}$ and the cyan dotted-dashed curve represents the lithium profile after an accretion of $1 M_{\oplus}$.

An accreted mass lower or equal to $0.6 M_{\oplus}$ does not have any real impact on the lithium abundance as it reduces its surface value by a factor lower than 10 percent. The mixing is not enough efficient to mix the lithium down to the destruction layers. For masses larger than $0.6 M_{\oplus}$, the lithium destruction becomes important and reaches a factor 3.5 for an accreted mass of $0.66 M_{\oplus}$ and more than a factor 100 for an accreted mass of $1 M_{\oplus}$.

Thus a small amount of planetary matter is enough to reduce significantly the lithium surface abundance in this type of stars.

After the accretion episode in 16 Cygni B, the lithium abundance goes on decreasing due to other extra mixing processes in the two stars as discussed in the previous section. We plotted in Fig. 7 the lithium surface abundance evolution with the assumption of an accretion episode of $0.66 M_{\oplus}$ (blue dotted line), which is enough to account for the observations. As the lithium observation in 16 Cygni B is only an upper limit, any accretion mass larger than this value can explain the abundance difference in the two stars.

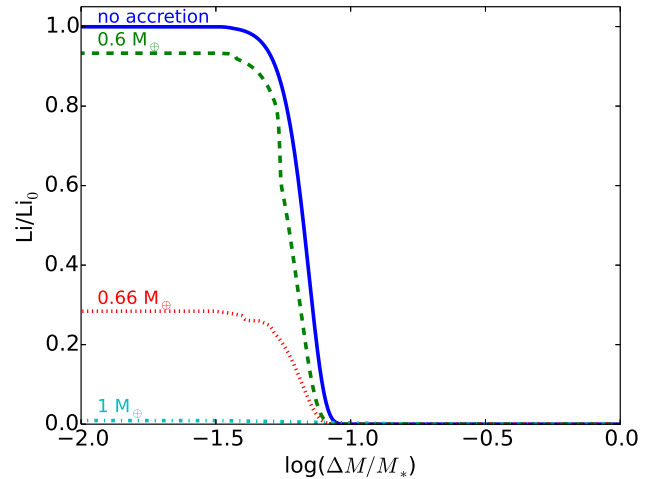


Fig. 9. Lithium abundance profiles after the accretion of different masses in the model of 16 Cygni B: no accretion (blue solid line), $0.6 M_{\oplus}$ (green dashed line), $0.66 M_{\oplus}$ (red dotted line) and $1 M_{\oplus}$ (cyan dotted-dashed line) at the beginning of the MS.

5.3. The beryllium case

Beryllium has been detected in 16 Cygni A and B by Deliyannis et al. (2000) who find that the difference between the two abundances, if any, must be smaller than 0.2 dex. Beryllium is destroyed by nuclear reactions at a temperature of $T \sim 3.5 \cdot 10^6 K$, larger than the lithium one. The fact that it is not depleted gives an upper limit on the accreted mass which must not lead to mixing down to its destruction region.

To characterise this effect we plotted the same figure as Fig. 9 for the beryllium (see Fig. 10). An important result is that for an accretion of $0.66 M_{\oplus}$ (red dotted line) the beryllium is not destroyed by nuclear reactions because fingering convection does not mix the stellar matter deep enough. However for an accretion of $1 M_{\oplus}$ (cyan dotted-dashed line) beryllium is already reduced by a factor 5. If the beryllium abundance determination of the two component of the 16 Cygni system is confirmed, it may lead to a precise determination of the accreted mass.

6. Summary and discussion

The 16 Cygni system is particularly interesting for comparative studies of stars with and without planets. The two main stars of this system have been observed in several ways, leading to very precise constraints.

The most striking feature is the lithium abundance, which is slightly larger than the solar one for 16 Cygni A and smaller by a factor at least 4.7 in 16 Cygni B (Friel et al. 1993; King et al. 1997). The lithium value given for this later star is in fact an upper limit, so that it could be completely lithium depleted.

In this paper, we have presented detailed computations of these two stars, leading to models which precisely fit their asteroseismic frequency determinations, as well as their radii, luminosities, effective temperatures and gravities. These models have been computed by fully taking into account atomic diffusion of helium and heavy elements. Their characteristics are given in Table 2.

Then we discussed the importance of the lithium observations for the two stars. We first showed that the very large lithium

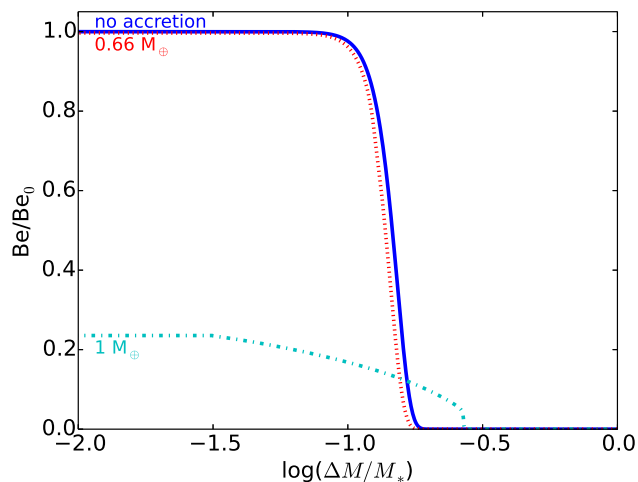


Fig. 10. Beryllium abundance profiles after the accretion of different masses: no accretion (blue solid line), $0.66 M_{\oplus}$ (red dotted line) and $1 M_{\oplus}$ (cyan dotted-dashed line) at the beginning of the MS.

depletion observed in 16 Cygni B cannot be accounted for by the classical means of rotational-induced mixing or similar types of extra mixing. The observable parameters difference between them is too small to explain such a large difference in lithium as observed. We suggest that the accretion of heavy matter onto the planet host star 16 Cygni B in its early main sequence phase induced a special kind of mixing, namely fingering convection, which lead to a large lithium destruction in a relatively small time-scale (c.f. Vauclair 2004; Théado & Vauclair 2012).

We recall that, when a star accretes heavy matter onto lighter one, the induced μ -gradient leads to a specific kind of hydrodynamical instability, called fingering convection or thermohaline convection, which mixes all the accreted matter downwards. Contrary to what is often assumed, the accreted heavy elements do not leave any signature in the stellar outer layers because of this mixing. On the other hand, the same mixing may transport lithium down to the layers where it is destroyed by nuclear reactions.

We suggest that, during the evolution of the planetary disk, at the beginning of the main sequence phase, 16 Cygni B may have swallowed a fraction of earth-like planet which have lead to fingering convection below the convective zone. This short-time efficient extra-mixing allowed the transport of lithium down to the nuclear destruction region. We have seen that two third of an earth-mass planet would be enough to account for the observed upper value of lithium in 16 Cyg B, as shown in Fig. 7. Observations of beryllium have been reported in these two stars by Deliyannis et al. (2000). They found no difference between them. If confirmed, it means that the accretion of planetary matter could not have been larger than one earth mass.

We also computed the detailed variations of the heavy elements abundances due to atomic diffusion, along the two evolutionary tracks leading to the best models for 16 Cygni A and B. Atomic diffusion alone leads to carbon depletion by about 0.05 dex and to magnesium depletion by about 0.03 dex. The resulting abundances in the two stars are very close, as observed by Schuler et al. (2011). Differences as suggested by Ramírez et al. 2011 and Tucci Maia et al. 2014 could not be explained in this context.

In summary, the 16 Cygni system gives evidence of fingering convection induced by the accretion of planetary matter, which is probably the unknown process invoked in the past by several authors to account for the large lithium differences between the two stars.

This result can be generalized to all planet-host stars, which may accrete planetary matter in a random way, with various accretion rates. As already suggested by Théado et al. (2012), this could lead to an average lithium abundance smaller in planet-host stars than in other stars, as claimed by Israelian et al. (2009) and Delgado Mena et al. (2014). In this framework, precise lithium abundances in seismically observed stars with or without observed planets would be very useful. Furthermore, beryllium observations in the same stars would help constraining the mass accreted onto the star.

Acknowledgements. We thank the "Programme National de Physique Stellaire" (PNPS) of CNRS/INSU (France) for his financial support. We also warmly thank Piercarlo Bonifacio for very useful comments on the first version of this paper.

References

- Alecian, G. & Leblanc, F. 2004, in IAU Symposium, Vol. 224, The A-Star Puzzle, ed. J. Zverko, J. Ziznovsky, S. J. Adelman, & W. W. Weiss, 587–589
- Allègre, C. J., Poirier, J.-P., Humler, E., & Hofmann, A. W. 1995, *Earth and Planetary Science Letters*, 134, 515
- Angulo, C. 1999, in American Institute of Physics Conference Series, Vol. 495, American Institute of Physics Conference Series, 365–366
- Brassard, P. & Charpinet, S. 2008, *Ap&SS*, 316, 107
- Brown, J. M., Garaud, P., & Stellmach, S. 2013, *ApJ*, 768, 34
- Castro, M., Vauclair, S., Richard, O., & Santos, N. C. 2009, *A&A*, 494, 663
- Charbonnel, C., Vauclair, S., Maeder, A., Meynet, G., & Schaller, G. 1994, *A&A*, 283, 155
- Charbonnel, C., Vauclair, S., & Zahn, J.-P. 1992, *A&A*, 255, 191
- Cochran, W. D., Hatzes, A. P., Butler, R. P., & Marcy, G. W. 1997, *ApJ*, 483, 457
- Davies, G. R., Chaplin, W. J., Farr, W. M., et al. 2015, *MNRAS*, 446, 2959
- Deal, M., Deheuvels, S., Vauclair, G., Vauclair, S., & Wachlin, F. C. 2013, *A&A*, 557, L12
- Deal, M., Richard, O., & Vauclair, S. 2015, in preparation
- Delgado Mena, E., Israelian, G., González Hernández, J. I., et al. 2014, *A&A*, 562, A92
- Deliyannis, C. P., Cunha, K., King, J. R., & Boesgaard, A. M. 2000, *AJ*, 119, 2437
- Denissenkov, P. A. 2010, *ApJ*, 723, 563
- Friel, E., Cayrel de Strobel, G., Chmielewski, Y., et al. 1993, *A&A*, 274, 825
- Garaud, P. 2011, *ApJ*, 728, L30
- Hauser, H. M. & Marcy, G. W. 1999, *PASP*, 111, 321
- Israelian, G., Delgado Mena, E., Santos, N. C., et al. 2009, *Nature*, 462, 189
- King, J. R., Deliyannis, C. P., Hiltgen, D. D., et al. 1997, *AJ*, 113, 1871
- Kippenhahn, R., Ruschenplatt, G., & Thomas, H.-C. 1980, *A&A*, 91, 175
- Kjeldsen, H., Bedding, T. R., & Christensen-Dalsgaard, J. 2008, *ApJ*, 683, L175
- Metcalfe, T. S., Chaplin, W. J., Appourchaux, T., et al. 2012, *ApJ*, 748, L10
- Paquette, C., Pelletier, C., Fontaine, G., & Michaud, G. 1986, *ApJS*, 61, 177
- Patience, J., White, R. J., Ghez, A. M., et al. 2002, *ApJ*, 581, 654
- Pinsonneault, M. H., Kawaler, S. D., & Demarque, P. 1990, *ApJS*, 74, 501
- Ramírez, I., Meléndez, J., & Asplund, M. 2009, *A&A*, 508, L17
- Ramírez, I., Meléndez, J., Cornejo, D., Roederer, I. U., & Fish, J. R. 2011, *ApJ*, 740, 76
- Richer, J., Michaud, G., & Turcotte, S. 2000, *ApJ*, 529, 338
- Rogers, F. J. & Nayfonov, A. 2002, *ApJ*, 576, 1064
- Schuler, S. C., Cunha, K., Smith, V. V., et al. 2011, *ApJ*, 737, L32
- Seaton, M. J. 2005, *MNRAS*, 362, L1
- Tassoul, M. 1980, *ApJS*, 43, 469
- Théado, S., Alecian, G., LeBlanc, F., & Vauclair, S. 2012, *A&A*, 546, A100
- Théado, S. & Vauclair, S. 2012, *ApJ*, 744, 123
- Torres, G. 2010, *AJ*, 140, 1158
- Traxler, A., Garaud, P., & Stellmach, S. 2011, *ApJ*, 728, L29
- Tucci Maia, M., Meléndez, J., & Ramírez, I. 2014, *ApJ*, 790, L25
- Turner, N. H., ten Brummelaar, T. A., McAlister, H. A., et al. 2001, *AJ*, 121, 3254
- Ulrich, R. K. 1972, *ApJ*, 172, 165
- van Leeuwen, F. 2007, *A&A*, 474, 653
- Vauclair, S. 1988, *ApJ*, 335, 971
- Vauclair, S. 2004, *ApJ*, 605, 874
- White, T. R., Huber, D., Maestri, V., et al. 2013, *MNRAS*, 433, 1262
- Zahn, J.-P. 1992, *A&A*, 265, 115
- Zemskova, V., Garaud, P., Deal, M., & Vauclair, S. 2014, *ApJ*, 795, 118